Cell, Vol. 105, 257–267, April 20, 2001, Copyright ©2001 by Cell Press

Crystal Structure of the 14-3-3ζ:Serotonin N-Acetyltransferase Complex: A Role for Scaffolding in Enzyme Regulation

Tomas Obsil,* Rodolfo Ghirlando,* David C. Klein,† Surajit Ganguly,† and Fred Dyda*‡

*Laboratory of Molecular Biology
National Institute of Diabetes and Digestive and Kidney Diseases
†Laboratory of Developmental Neurobiology
National Institute of Child Health and Human Development
National Institutes of Health
Bethesda, Maryland 20892

Summary

Serotonin N-acetyltransferase (AANAT) controls the daily rhythm in melatonin synthesis. When isolated from tissue, AANAT copurifies with isoforms ε and ζ of 14-3-3. We have determined the structure of AANAT bound to 14-3-3ζ, an association that is phosphorylation dependent. AANAT is bound in the central channel of the 14-3-3ζ dimer, and is held in place by extensive interactions both with the amphipathic phosphopeptide binding groove of 14-3-3ζ and with other parts of the central channel. Thermodynamic and activity measurements, together with crystallographic analysis, indicate that binding of AANAT by 14-3-3ζ modulates AANAT's activity and affinity for its substrates by stabilizing a region of AANAT involved in substrate binding.

Introduction

An important feature of biological systems is the capacity to generate endogenous circadian rhythms coordinated with the 24 hr environmental lighting cycle (reviewed in Reppert, 1998; Dunlap, 1999). A key output signal of the vertebrate circadian system is melatonin (5-methoxy-N-acetyltryptamine); circulating levels of melatonin increase 10-fold at night. Melatonin is thought to function both as a downstream signal and as a feedback signal for the biological clock (Klein et al., 1991; Arendt, 1995). The oscillator that drives the melatonin rhythm and coordinates other aspects of circadian physiology is the suprachiasmatic nucleus (SCN) of the hypothalamus—the Mind's Clock. Light acting through the retina and a retinal→hypothalamic pathway entrains the circadian rhythm of the SCN with the environmental day-night cycle. A neural pathway connects the SCN to the pineal gland; at night, norepinephrine is released by sympathetic nerves, resulting in receptor-mediated elevation of cAMP. This second messenger is critical in regulating the synthesis of melatonin.

cAMP regulates melatonin production by controlling the activity of the penultimate enzyme in melatonin synthesis, serotonin N-acetyltransferase (arylalkylamine N-acetyltransferase; AANAT). AANAT catalyzes acetyl transfer from acetyl-coenzyme A (AcCoA) to serotonin, yielding N-acetylserotonin, the precursor of melatonin. This enzyme belongs to the GNAT superfamily (*G*CN5-related *N-a*cetyl*t*ransferase) (Neuwald and Landsman, 1997; Dyda et al., 2000).

cAMP acts through multiple mechanisms to control AANAT activity, the prominence of each varying from species to species (Klein et al., 1998). For example, in rodents, cAMP directs a large increase in AANAT mRNA, which is essential for increased AANAT activity (Roseboom et al., 1996; Klein et al., 1997); cAMP also acts to block proteasomal proteolysis of AANAT (Gastel et al., 1998). This latter mechanism appears to play a dominant role in other species such as sheep, where AANAT mRNA levels are essentially constant. cAMP also appears to activate AANAT in intact cells (Namboodiri et al., 1985; Thibault et al., 1993; S. Coon and D. C. K., unpublished data).

Biochemical and structural studies have provided insight into the molecular mechanism through which AANAT catalyzes acetyl transfer to serotonin. The three-dimensional structures of a fully active but truncated form of ovine AANAT, $AANAT_{28–201}$, have been recently determined in the apo form and also as a complex with CoA-S-acetyltryptamine (Hickman et al., 1999a, 1999b). This bisubstrate analog is a potent inhibitor that closely approximates the apparent catalytic intermediate (Khalil and Cole, 1998). Comparison of the two structures revealed a dramatic conformational change upon binding of the bisubstrate analog affecting an 18-residue region. This reorganization has two effects: it allows AcCoA access to its binding site, and structurally completes the binding site for serotonin. This finding provided a clear structural explanation for kinetic results indicating ordered substrate binding in which AcCoA binding precedes serotonin binding (De Angelis et al., 1998).

The structural studies of AANAT were done using $AANAT_{28–201}$ because it was not possible to obtain diffraction quality crystals of full-length $AANAT_{1–207}$. The missing sequences at the N and C termini include highly conserved motifs that contain phosphorylation sites for the cAMP-dependent protein kinase, PKA (Coon et al., 1995). Furthermore, the N-terminal PKA site is embedded within a putative binding site for 14-3-3 proteins (Aitken, 1996).

14-3-3 proteins form a highly conserved family of homo- and heterodimeric proteins (Aitken, 1996; Fu et al., 2000). Seven highly homologous isoforms have been identified in mammals, and several other isoforms are found in plants, yeast, and fungi (Finnie et al., 1999). The 14-3-3 proteins are ubiquitously expressed and are abundant; for example, they comprise 1% of total soluble protein in the brain (Boston et al., 1982). Although a single conserved cellular function of 14-3-3 proteins is not apparent, an important common characteristic is their ability to bind to other proteins; over 50 such examples exist. Through these binding reactions, the 14-3-3 proteins appear to act as molecular scaffolds or

‡To whom correspondence should be addressed (e-mail: dyda@ulti.niddk.nih.gov).

chaperones. Biological roles of 14-3-3 complexes have been demonstrated in signal transduction, subcellular targeting, and cell cycle control. 14-3-3 proteins can also act as allosteric cofactors modulating the catalytic activity of their binding partners (e.g., Tanji et al., 1994; Banik et al., 1997; Thorson et al., 1998). It has also been suggested that 14-3-3 proteins may bring together two different signaling molecules to modulate each other's activity (Braselmann and McCormick, 1995; Vincenz and Dixit, 1996).

14-3-3 proteins bind to discrete phosphoserine (pSer) or phosphothreonine (pThr) containing motifs, present in most known 14-3-3 binding proteins (Aitken, 1996; Muslin et al., 1996; Yaffe et al., 1997; Fu et al., 2000). AANATs contain a conserved sequence motif, [RRHTLP] (residues 28–33 of ovine AANAT), that is similar to the canonical motifs, [RSXpSXP; RXY/FXpSXP], described by Yaffe et al. (1997) and Rittinger et al. (1999).

A functional relationship between AANAT and the ζ and ϵ isoforms of 14-3-3 was first indicated by the observation that these proteins copurify through multiple chromatography steps as an ~80 kDa complex (Roseboom et al., 1994). It was subsequently shown that AANAT is phosphorylated in the cell at the N-terminal PKA site (Gastel et al., 1998), and that recombinant AANAT binds to 14-3-3 only when AANAT is phosphorylated at Thr-31 (J. Gastel, S. G., and D. C. K., unpublished data).

Crystal structures of the ζ and τ isoforms of 14-3-3 have been determined (Liu et al., 1995; Xiao et al., 1995), as have structures of 14-3-3ζ bound to various peptides representing 14-3-3 binding motifs (Yaffe et al., 1997; Petosa et al., 1998; Rittinger et al., 1999). In these structures, 14-3-3 monomers, each composed of nine antiparallel α helices, form homodimers with a large, deep channel in the center running the length of the dimer. The walls of the channel contain amphipathic grooves that are ~30 Å long. pSer-containing peptides were observed to bind in an extended conformation within these grooves. The structures suggested the enticing possibility that the channel can sequester proteins or domains of proteins.

We present here the three-dimensional structure of the complex between 14-3-3ζ and serotonin N-acetyltransferase with a bound bisubstrate analog, determined at 2.7 Å resolution. This structure allows us to describe how 14-3-3 interacts with an enzymatically active protein, and supports the hypothesis that 14-3-3ζ modulates AANAT function by maintaining an AANAT conformation that enhances substrate binding. To test this hypothesis, we performed isothermal titration calorimetry and activity measurements to compare the uncomplexed and the 14-3-3 bound forms of AANAT.

Results and Discussion

Biophysical Characterization of 14-3-3ζ:pAANAT Complexes

Our initial attempts at crystallization focused on full-length ovine AANAT and 14-3-3ζ. Recombinantly expressed $AANAT_{1–207}$ was phosphorylated in vitro at both PKA sites, Thr-31 and Ser-205. When doubly phosphorylated $AANAT_{1–207}$ ($dpAANAT_{1–207}$) was mixed with twice the stoichiometric amount of 14-3-3ζ (unless otherwise stated, moles are of monomers), gel filtration experiments demonstrated that all the protein eluted as a single peak of ~80 kDa. The stoichiometry and monodispersity of this complex were confirmed using sedimentation equilibrium measurements that gave 75.9 ± 2.0 kDa as its molecular mass. This corresponds to the sum of the molecular masses for $dpAANAT_{1–207}$ (23.2 kDa) and the 14-3-3ζ dimer (56.0 kDa). Increasing the relative concentration of $dpAANAT_{1–207}$ to 14-3-3ζ did not change the stoichiometry of the complex. To date, we have been unable to obtain diffracting crystals of this 2:1 complex.

Previous work demonstrated that $AANAT_{1–201}$ exhibited far better solution properties than full-length AANAT (Hickman et al., 1999a). We therefore reasoned that the last six C-terminal residues might be disordered in the complex, preventing crystallization. When ovine $AANAT_{1–201}$ is phosphorylated at Thr-31 by PKA, it binds to 14-3-3ζ, but depending on the relative ratios of the two proteins, two complexes of differing stoichiometry can be obtained. Sedimentation equilibrium measurements indicated that at a 2:1 mixing ratio of 14-3-3ζ to $pAANAT_{1–201}$, a complex with 2:1 stoichiometry is exclusively formed. Data analysis leads to a $K_{D1} = K_{D2}$ of ~20 nM. At a 2:2 mixing ratio, a complex with 2:2 stoichiometry is formed whose stability is buffer-dependent.

Table 1. Data Collection and Refinement Statistics

Data Collection	
Resolution (Å)	20–2.7
Total reflections (N)	78,001
Unique reflections (N)	44,944
Completeness (%) (for I/σ (I) > 0.0)	84.9
I/σ (I)	5.5
R_{sym}	0.102
Highest shell (between 2.78–2.70 Å):	
Completeness (%)	72
I/σ (I)	2.09
R_{sym}	0.251
Refinement	
Resolution (Å)	20–2.7
Atoms (N)	13,479
Reflections $F > 1\sigma$ (F)	44,626
R factor (%)	20.4
R_{free} (%)	22.8
Rms bond lengths (Å)	0.008
Rms bond angles (°)	1.55
Average B factor (Å^2)	16.3
Average rms B factor bonded atoms (Å^2)	2.29

$R_{sym} = \Sigma|I - <I>|/\Sigma<I>$
R factor $= \Sigma|FP_o - FP_c|/\Sigma|FP_o|$
R_{free} is computed using 5% of the total reflections selected randomly and never used in refinement.

Structure Determination

X-ray diffraction quality crystals were obtained with 14-3-3ζ and $pAANAT_{1–201}$ that was first complexed with CoA-S-acetyl tryptamine. For crystallization trials, 14-3-3ζ and $pAANAT_{1–201}$ were mixed at a 2:1 molar ratio (see Experimental Procedures). The structure of the complex was solved using molecular replacement, which indicated exclusively 2:2 complexes. The structure was subsequently refined at 2.7 Å resolution (see Experimental Procedures and Table 1). The crystals are in the triclinic space group and contain two 14-3-3ζ dimers, each of

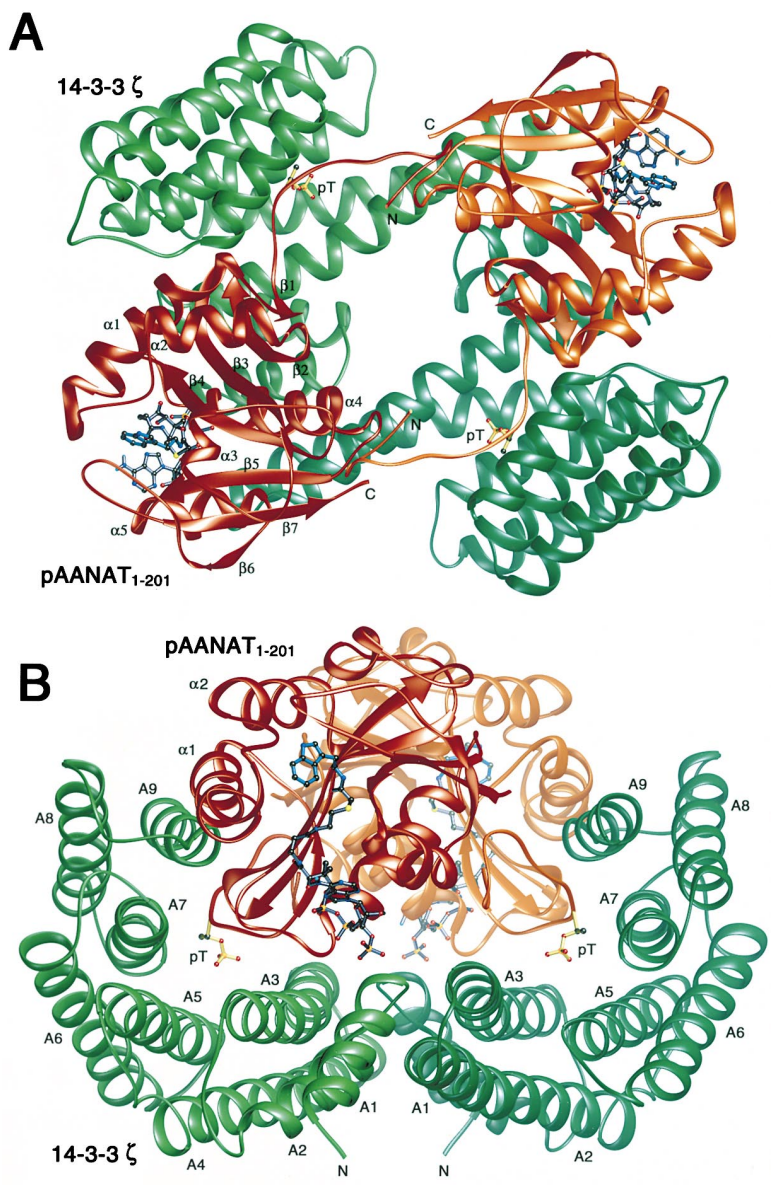

Figure 1. Structure of the 14-3-3ζ:pAANAT$_{1-201}$ Complex

(A) The 14-3-3ζ homodimer is shown in green, and the pAANAT$_{1-201}$ molecules in brown. The phosphorylated Thr-31 residue of pAANAT$_{1-201}$, pT, is shown in yellow, and the bisubstrate analog in blue.

(B) View rotated by 90° about the horizontal axis and 45° about the vertical axis.

which has two bound pAANAT$_{1-201}$ molecules. The structure therefore shows four crystallographically independent views of the interactions between a 14-3-3ζ monomer and pAANAT$_{1-201}$.

Overall Structure of the 14-3-3ζ:pAANAT$_{1-201}$ Complex

The crystal structure of the 14-3-3ζ:pAANAT$_{1-201}$ complex shows that each monomer of the 14-3-3 dimer binds one molecule of pAANAT$_{1-201}$ (Figure 1). The pAANAT$_{1-201}$ molecules occupy most of the central space in the channel of the 14-3-3 dimer. Residues of pAANAT$_{1-201}$ upstream of Ala-34 lead away from the core of pAANAT$_{1-201}$ and lie in an extended conformation in the amphipathic binding groove of 14-3-3ζ with the phosphate group of pThr-31 pointing into the positively charged depression in the middle of the groove, consistent with the observations made with phosphopeptides (Yaffe et al., 1997; Rittinger et al., 1999).

In addition to interactions involving pAANAT$_{1-201}$ residues flanking pThr-31, there are extensive interactions between pAANAT$_{1-201}$ and 14-3-3ζ that are remote from the phosphorylated residue. However, pAANAT$_{1-201}$ does not bridge 14-3-3ζ monomers (Figure 1B), and interactions are limited to those involving one monomer of 14-3-3ζ and the pAANAT$_{1-201}$ molecule whose pThr-31 is bound to that monomer. Other regions of pAANAT$_{1-201}$ that interact with 14-3-3ζ include the surface of helix α1, the turn between strands β2 and β3, and the loop between strand β4 and helix α4. (Greek letters identify the α helices of pAANAT$_{1-201}$ and capital letters those of 14-3-3ζ.) The C terminus of one pAANAT$_{1-201}$ molecule is directed toward the N terminus of the second (Figure 1A).

The total solvent-excluded surface area between a monomer of 14-3-3ζ and pAANAT$_{1-201}$ is 2527 Å^2 (Connolly, 1983). The extended N terminus of pAANAT$_{1-201}$ containing pThr-31 (Ser-18 to Ala-34) contributes ~41%

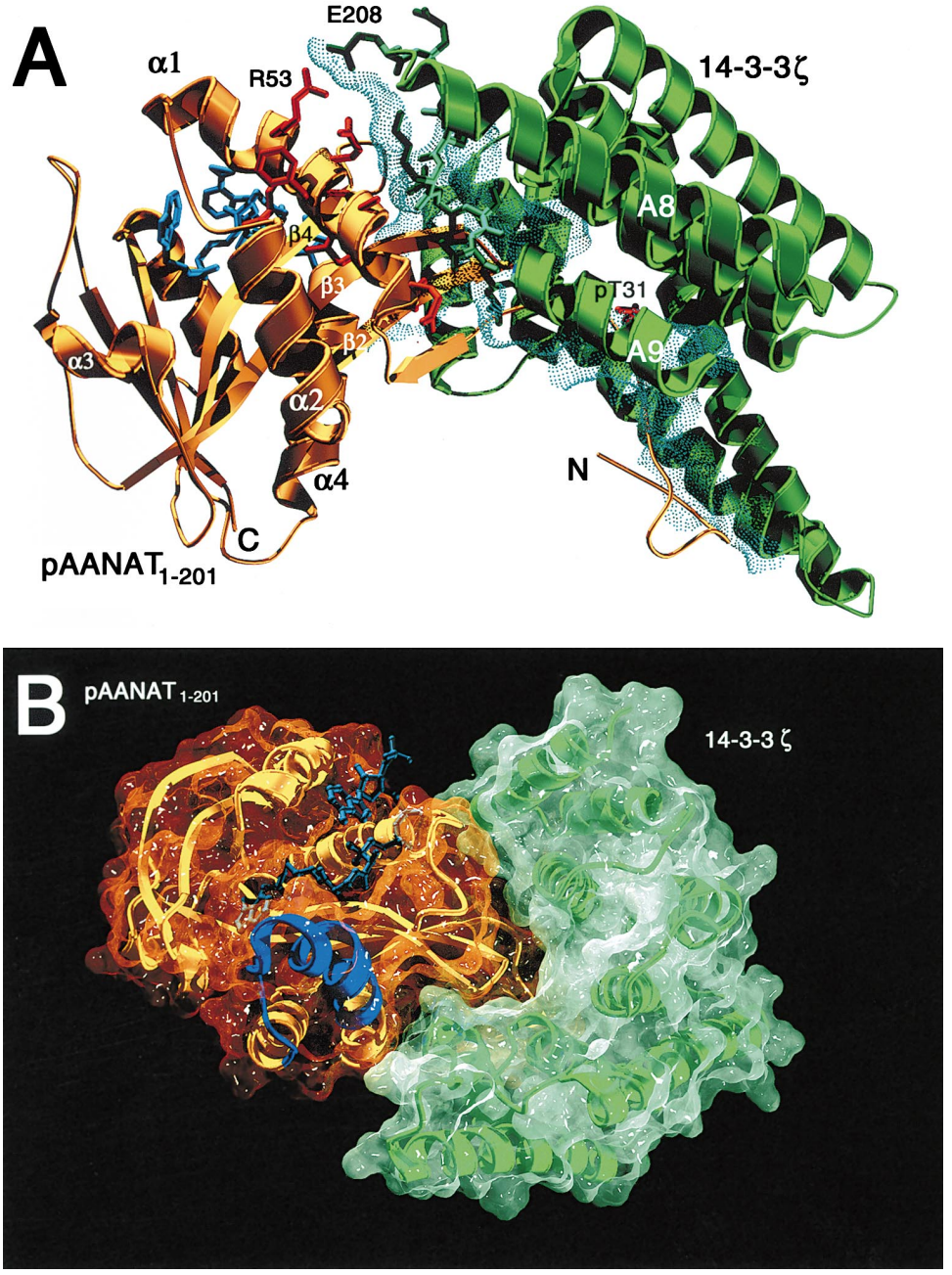

Figure 2. Interaction Between pAANAT$_{1-201}$ and a Monomer of 14-3-3ζ

(A) The solvent accessible surface of 14-3-3ζ that is buried upon complex formation with pAANAT$_{1-201}$ is shown as blue dots. Note that only ~41% of the contact region between the two proteins is contributed by the extended phospho-containing segment of pAANAT$_{1-201}$ and its binding groove (bottom right). The rest is contributed by other regions of 14-3-3ζ. The loop connecting helices A8 and A9 of 14-3-3ζ is shown as a stick model, with side chains in dark green. Side chains of residues on pAANAT$_{1-201}$ are shown in red.

(B) pAANAT$_{1-201}$ (in orange) is shown with the bound bisubstrate analog (in light blue) and the 14-3-3ζ monomer (in green). The 18 residues undergoing the conformational change upon substrate binding are shown in darker blue.

of the interface, while the rest is contributed by other parts of pAANAT$_{1-201}$ (Figure 2A). These combined interactions result in a three-dimensionally well-defined association between 14-3-3ζ and pAANAT$_{1-201}$.

The four crystallographically independent structures of a 14-3-3ζ monomer with one bound pAANAT$_{1-201}$ are essentially identical despite four different crystal packing environments. When the four 14-3-3ζ molecules in the asymmetric unit are superimposed (rms deviation in Cα positions is 0.22 Å), the resulting alignment superimposes the bound pAANAT$_{1-201}$ molecules with an rms deviation in Cα positions of 0.15 Å.

The structure of the core of pAANAT$_{1-201}$ in the complex is very similar to the previously described structure of

$AANAT_{28–201}$ complexed with the bisubstrate analog (Hickman et al., 1999b): the two structures can be aligned over 166 Cα atoms with an rms deviation of 0.17 Å. On the level of the 14-3-3ζ monomer, there are no major differences between the phosphopeptide complexes of 14-3-3ζ and the $pAANAT_{1–201}$-bound form. For example, the structure of a monomer of 14-3-3ζ complexed with $pAANAT_{1–201}$ can be superimposed on that of Rittinger et al. (1999; PDB code 1qja) with an rms deviation of only 0.64 Å over 214 Cα positions. The most significant difference affecting the 14-3-3ζ monomer involves the loop connecting its last two C-terminal helices, A8 and A9, most likely due to the direct interaction between this loop and α1 of $pAANAT_{1–201}$.

Despite the overall similarities of 14-3-3ζ monomers in the free and complexed forms, we do see differences in the 14-3-3ζ dimer that are most likely a consequence of $pAANAT_{1–201}$ binding. With respect to the phosphopeptide complexes of 14-3-3ζ, the central channel of 14-3-3ζ bound to $pAANAT_{1–201}$ opens up as a result of a rigid body rotation of the monomers. This rotation pivots on the axis of A5 that is near to the center of mass of the monomer, and causes the most distant α carbons on A8 to move by ~2 Å outward from the channel. The rotation also raises the floor of the channel by ~1.5 Å. Despite these movements, the 14-3-3ζ dimer of Rittinger et al. (1999) and that bound to $pAANAT_{1–201}$ can be superimposed with an rms deviation of 1.09 Å over 426 Cα positions.

In the complex, the N-terminal region of $pAANAT_{1–201}$ interacts with the second $pAANAT_{1–201}$ molecule bound to the same 14-3-3 dimer (Figure 1A). This interaction stabilizes the chain allowing us to trace the polypeptide until Ser-18. Beyond this, the electron density map is too weak to interpret, presumably due to disorder.

Interactions between 14-3-3ζ and $pAANAT_{1–201}$ in the Phosphopeptide Binding Groove

The main chain conformation of the AANAT residues in the 14-3-3 binding groove, [RRHpTLPAN] (pT, pThr-31), is very similar to those seen in the complexes of 14-3-3ζ with phosphopeptides (Yaffe et al., 1997; Rittinger et al., 1999). The polypeptide chain of $pAANAT_{1–201}$ around pThr-31 adopts an extended conformation (Figure 3) that is most similar to that of the phosphopeptide with the "mode 2" consensus sequence, [RXY/FXpSXP], although its sequence is closer to the "mode 1" sequence, [RSXpSXP] (Rittinger et al., 1999).

The key interaction for 14-3-3ζ:$pAANAT_{1–201}$ association, coordination of pThr-31, is similar to the pSer coordination in the 14-3-3ζ:phosphopeptide complex structures (Figures 3B and 3C; Yaffe et al., 1997; Rittinger et al., 1999). Comparison of the available complexes indicates that an Arg at either the −2 and −4 position relative to the phosphorylated residue (seen in $pAANAT_{1–201}$ and the "mode 2" phosphopeptide, respectively) can act in the same way: salt bridging to both Glu-180 of 14-3-3ζ and the phosphate group. Interestingly, Arg-28 at the −3 position of $pAANAT_{1–201}$ is not directly involved in salt bridges, but the side chain electron density is unambiguous. In all three structures, Pro at the +2 position appears to force a change in the direction of the polypeptide chain.

Beyond the consensus 14-3-3 binding motif, only Asn-35 of the N-terminal region of $pAANAT_{1–201}$ interacts with 14-3-3ζ via hydrogen bonds. As this residue is not conserved in other proteins that interact with 14-3-3, this is probably an AANAT-specific bond. On the basis of this structure, the eight residue sequence, RRHpTLPAN from Arg-28 to Asn-35 (i.e., −3 to +4 with respect to pThr-31), constitutes the region of $pAANAT_{1–201}$ that interacts with the 14-3-3ζ binding groove.

The CG methyl group of pThr-31 (the only structural difference between Thr and Ser) is easily accommodated by 14-3-3ζ, where its closest contact is the CG1 methyl group of Val-172 of 14-3-3ζ. The two methyl groups are separated by ~4.0 Å, a distance commonly seen in hydrophobic protein cores. Since Val-172 is well conserved in the different 14-3-3 isoforms, Thr should be a good phosphate group carrier for binding to other isoforms as well. Although pSer is the more common phosphorylated residue in 14-3-3 binding proteins identified to date, FKHRL1, a member of the Forkhead family of transcription factors, also binds to 14-3-3ζ in a pThr-dependent manner (Brunet et al., 1999).

Beyond the Phosphopeptide: Other 14-3-3ζ:$pAANAT_{1–201}$ Interactions

There are extensive interactions between $pAANAT_{1–201}$ and 14-3-3ζ beyond those involving the 14-3-3 binding groove. The interactions within the binding groove involve a segment of $pAANAT_{1–201}$ that is probably disordered when it is not bound to 14-3-3, a notion supported by its protease sensitivity (Hickman et al., 1999a). In contrast, the other interacting regions of both molecules are contributed by elements that independently possess defined tertiary structure. As a consequence, 14-3-3ζ and $pAANAT_{1–201}$ are in a stable three-dimensional configuration relative to each other.

In terms of $pAANAT_{1–201}$, major contributions to the interface arise from the first two turns of helix α1, the turn between strands β2 and β3, and the loop between β4 and α4 (Figure 1). The faces of 14-3-3 helices A1, A3, A5, A7, and A9 pointing into the central channel all contribute to this region of the interface. As shown in Figure 2B, an extensive protruding surface of $pAANAT_{1–201}$ fits snugly against 14-3-3ζ, an interaction that includes hydrophobic contacts. In contrast, the interactions between 14-3-3ζ and the $pAANAT_{1–201}$ N-terminal phosphopeptide region involve mostly polar contacts. This distinction is not surprising, as it is reasonable to employ specific polar contacts for binding of the conserved sequence motif. The use of less specific hydrophobic contacts for the rest of the interface may allow 14-3-3 molecules to bind different partners in a structurally similar way—utilizing the inside surface of the channel—while allowing disparate complexes to differ in the exact atomic details of the interactions.

In both regions comprising the interface between $pAANAT_{1–201}$ and 14-3-3ζ, all the residues of 14-3-3ζ that are involved are highly conserved in the different isoforms. Of the 37 residues of 14-3-3ζ that contact $pAANAT_{1–201}$, 34 are identical among the 49 sequences (representing 7 isoforms) in the Swiss-Prot database. The four others are conservatively substituted. This reflects the fact that the inside of the channel is lined with highly conserved

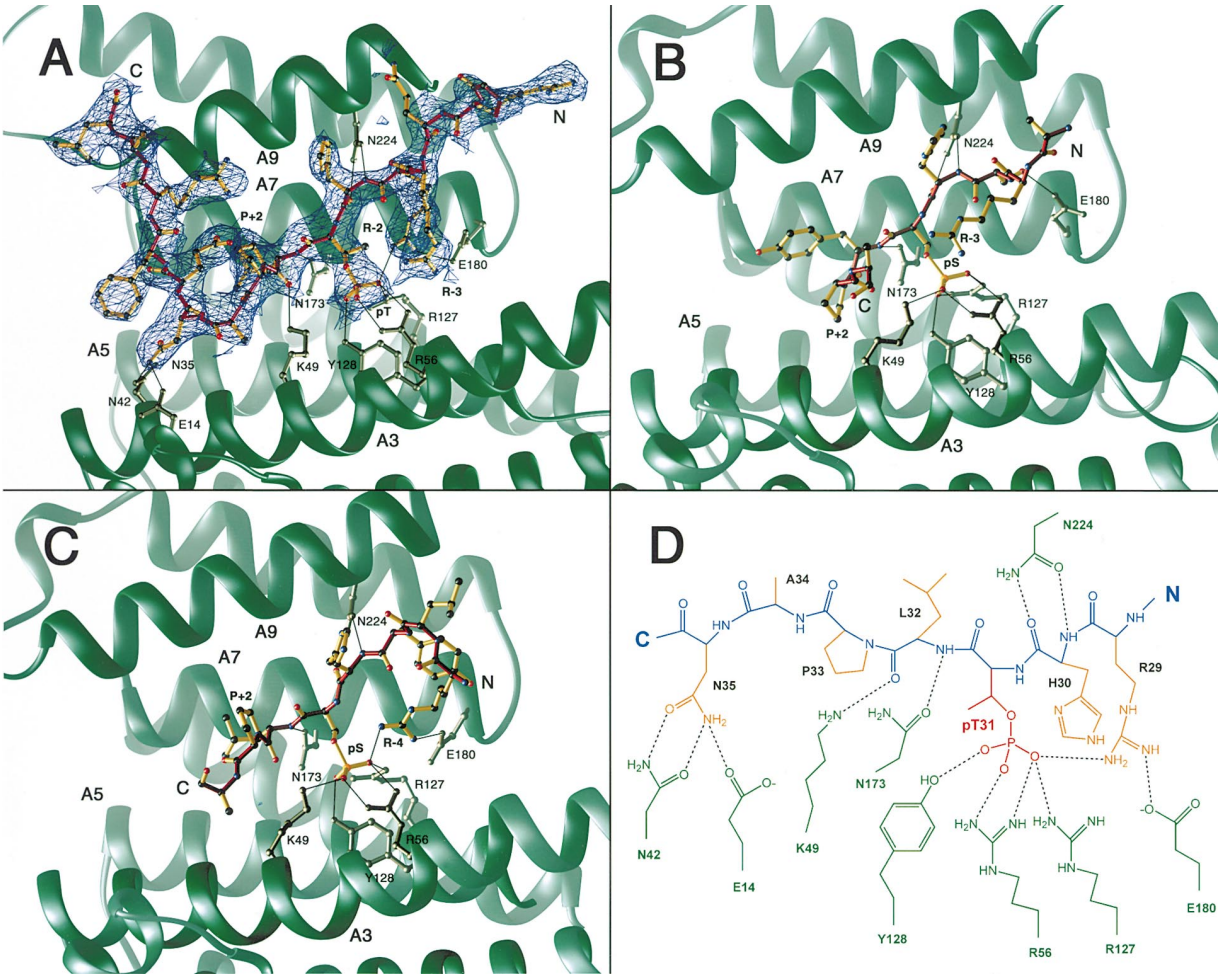

Figure 3. Comparison of the 14-3-3ζ:pAANAT$_{1–201}$ and 14-3-3:Phosphopeptide Complexes

(A) Contacts between 14-3-3ζ and the N-terminal region of pAANAT$_{1–201}$ (residues Arg-26 to Leu-40 containing phosphothreonine-31, pT). The averaged composite of all omit 2Fo−Fc electron density map is contoured at 0.8σ. The main chain of pAANAT$_{1–201}$ is shown in red. The phosphate group of Thr-31 is coordinated by Arg-56, Tyr-128, and Arg-127 of 14-3-3ζ, and Arg-29 of pAANAT$_{1–201}$.

(B) The "mode 1" phosphopeptide, [ARSHpSYPA], of Rittinger et al. (1999) bound to 14-3-3ζ.

(C) The "mode 2" phosphopeptide, [RLYHpSLPA], of Rittinger et al. (1999) bound to 14-3-3ζ.

(D) Schematic diagram of the contacts between 14-3-3ζ and the N terminus of pAANAT$_{1–201}$.

residues (Liu et al., 1995; Xiao et al., 1995). Although this observation suggests that pAANAT$_{1–201}$ might interact equally well with other isoforms of 14-3-3, the initial copurification experiments from pineal tissue indicated enrichment only with the ε and ζ isoforms, which are not the dominant isoforms in sheep pineal homogenates (Roseboom et al., 1994). The sheep and human 14-3-3ζ differ only by one residue (Ala-112 in human versus Pro-112 in sheep) which is not located in the interface.

Implications of Complex Formation for AANAT Catalysis

Previous structural work revealed a substantial conformational rearrangement affecting AANAT upon binding the bisubstrate analog (Hickman et al., 1999a, 1999b), providing a structural basis for its ordered substrate binding. The 18 residues affected by this structural change comprise loop 1 and are located at the carboxyl end of α1 and the region connecting α1 and α2. In uncomplexed AANAT, α1 is eight residues long and is followed by an extended loop and then a short β strand that occupies part of the AcCoA binding site, mimicking the panthetheine moiety of AcCoA. When complexed with the bisubstrate analog, α1 becomes twice as long and has a slightly shifted orientation; as a result, the polypeptide following α1 exits the AcCoA binding site and instead forms one wall of the serotonin binding pocket.

It is intriguing that the regions of pAANAT$_{1–201}$ that interact with 14-3-3ζ include those involved in the conformational change upon substrate binding (Figure 2A). It is also clear that the substrate-free form of AANAT$_{1–201}$ cannot be docked directly to 14-3-3ζ, due to steric clashes with α1 and the extended loop following it. The structure of the complex suggested the possibility that binding of 14-3-3 may force pAANAT$_{1–201}$ to adopt a conformation that allows both substrates easy access to their binding sites.

To investigate the effect of 14-3-3ζ binding on the affinity of AANAT for its substrates, we performed iso-

Table 2. Thermodynamic Parameters of AcCoA and Serotonin Binding to Uncomplexed and Complexed pAANAT with 14-3-3ζ

Acetyl-Coenzyme A	K_D (μM)	ΔH (kcal/mol)	ΔG (kcal/mol)[a]	TΔS (kcal/mol)
$dpAANAT_{1-207}$	242 ± 3	−14.1 ± 0.8	−4.9 ± 0.1	−9.2 ± 0.9
14-3-3:$dpAANAT_{1-207}$ (2:1)	59 ± 8	−2.3 ± 0.1	−5.7 ± 0.1	3.4 ± 0.3
$pAANAT_{1-201}$	364 ± 35	−19.7 ± 4.2	−4.7 ± 0.1	−15 ± 4.2
14-3-3:$pAANAT_{1-201}$ (2:1)	71 ± 1	−6.3 ± 0.5	−5.6 ± 0.1	−0.7 ± 0.6
Serotonin[b]				
$dpAANAT_{1-207}$	1299 ± 115	−11.8 ± 2.1	−3.9 ± 0.1	−7.9 ± 2.2
14-3-3:$dpAANAT_{1-207}$ (2:1)	234 ± 4	−11.1 ± 0.1	−4.9 ± 0.1	−6.2 ± 0.2
$pAANAT_{1-201}$	1193 ± 177	−10.1 ± 0.9	−3.9 ± 0.2	−6.2 ± 0.9
14-3-3:$pAANAT_{1-201}$ (2:1)	350 ± 24	−10.5 ± 0.4	−4.7 ± 0.1	−5.8 ± 0.4

All values correspond to the mean of 2–3 experiments.
[a] ΔG and ΔS values were calculated using $\Delta G = -RT \ln K_a = \Delta H - T\Delta S$
[b] Serotonin binding measurements were performed in the presence of 5 mM CoA

thermal titration calorimetry (ITC) measurements. As shown in Table 2, when complexed with 14-3-3ζ, phosphorylated AANAT has a significantly improved binding affinity (indicated by the decrease in the dissociation constants, K_D) for both AcCoA (Figure 4) and serotonin. In terms of the Gibbs free energy, ΔG, complex formation

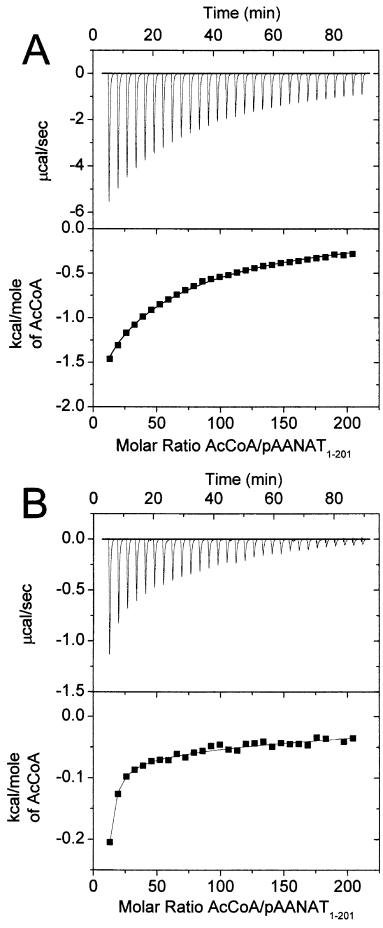

Figure 4. Isothermal Titration Calorimetry of AcCoA Binding to $pAANAT_{1-201}$

(A) Measurement of the interaction of AcCoA with $pAANAT_{1-201}$ alone. The upper panel shows the heat effect upon titration of 12 μM $pAANAT_{1-201}$ with 20 mM AcCoA. The lower panel represents the binding isotherm and the best-fit curve.

(B) Measurement of the interaction of AcCoA with the 14-3-3ζ:$pAANAT_{1-201}$ complex (24 μM 14-3-3ζ and 12 μM $pAANAT_{1-201}$).

of either $dpAANAT_{1-207}$ or $pAANAT_{1-201}$ with 14-3-3ζ facilitates AcCoA binding by ~0.8 kcal/mol. This improvement is a result of favorable entropy changes (in TΔS) that more than compensate for less favorable enthalpy changes (in ΔH). For the uncomplexed phosphorylated AANATs, the large negative values of TΔS for AcCoA binding are consistent with the observed conformational changes associated with AcCoA binding. In contrast, when AANAT is bound to 14-3-3ζ, the significantly less negative values in TΔS for AcCoA binding very likely reflect a more ordered conformation of the enzyme, suggesting that AcCoA binding is not accompanied by a dramatic change in conformation (Hinz, 1983; Sutherland and Aust, 1997).

The ITC data also show that the 14-3-3ζ complexed forms of phosphorylated AANATs have significantly increased affinity for serotonin when compared with the uncomplexed forms (Table 2). In contrast with AcCoA binding, however, there are no major differences in either ΔH or TΔS. It is notable that the approximately 5-fold effect on serotonin binding affinity that we measure is comparable to the fluctuation in serotonin concentrations in the sheep pineal gland (Namboodiri et al., 1985).

Further ITC measurements were performed to see if the ordered binding kinetics of AANAT alone were maintained in the complex. The data indicated that, as with free AANAT, the binding affinity of complexed phosphorylated AANAT for serotonin was negligible in the absence of AcCoA (data not shown).

The 14-3-3ζ bound pAANAT is enzymatically active, allowing us to perform activity measurements to compare the properties of complexed and free phosphorylated AANAT. Under the assay conditions used, in which substrates are below the Km of the enzyme, the addition of 14-3-3ζ stimulates the activity of both $pAANAT_{1-201}$ and $dpAANAT_{1-207}$ relative to the uncomplexed proteins. The maximal stimulation is ~60% relative to the unphosphorylated versions of AANAT in the presence of 14-3-3ζ (Figure 5). This improvement is on the same order as the ~45% increase in activity of tryptophan hydroxylase upon complex formation with 14-3-3 (Banik et al., 1997), and the 2- to 3-fold stimulation of protein kinase C by 14-3-3 (Tanji et al., 1994). Half-stimulation occurs at a molar ratio of ~1.2:1 14-3-3ζ dimer to $pAANAT_{1-201}$. Assuming a Kd value of 20 nM, half of the $pAANAT_{1-201}$ would be bound at a molar ratio of 1.3:1.

Previous studies have determined that binding of phosphorylated $AANAT_{1-207}$ to 14-3-3 lowers the Km for indole amines relative to that of uncomplexed $AANAT_{1-207}$

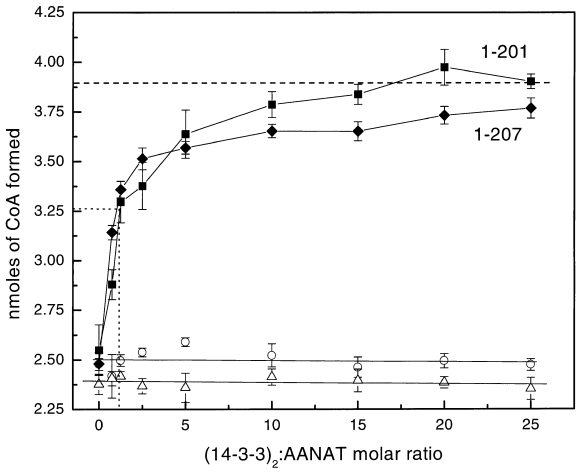

Figure 5. Activation of $pAANAT_{1-201}$ and $dpAANAT_{1-207}$ by Increasing Amounts of 14-3-3ζ

The activities of $pAANAT_{1-201}$ (square), $dpAANAT_{1-207}$ (diamond), nonphosphorylated $pAANAT_{1-201}$ (circle), and nonphosphorylated $pAANAT_{1-207}$ (triangle) were measured as a function of increasing amounts of 14-3-3ζ. There is no difference in activity between the nonphosphorylated and phosphorylated forms of AANAT in the absence of 14-3-3ζ.

(J. Gastel, S. G., and D. C. K., unpublished data). Collectively, the activity results and ITC data suggest that complex formation with 14-3-3ζ allows AANAT to bind its substrates more tightly, which under suitable assay conditions leads to increased product formation. This interpretation is supported by the structure of the complex, which indicates that 14-3-3ζ stabilizes the conformation of α1 and the loop following it in a configuration that enhances substrate binding.

In the crystal structure, the C terminus of the $pAANAT_{1-201}$ monomer bound to one monomer of 14-3-3ζ is directed toward the phosphopeptide binding groove of the other monomer within the 14-3-3 dimer (Figure 1A). The C terminus of AANAT (RRNSDR, residues 202–207) contains a PKA phosphorylation site at Ser-205. Although this sequence resembles canonical 14-3-3 binding motifs, binding experiments performed with phosphorylated peptides consisting of sequences from the AANAT N or C terminus indicate that binding of the phosphorylated C terminus of $dpAANAT_{1-207}$ by 14-3-3ζ is significantly weaker than that of the N terminus (see Experimental Procedures). However, the observation that 14-3-3ζ and $dpAANAT_{1-207}$ form exclusively 2:1 complexes indicates that although the phosphorylated C terminus of $dpAANAT_{1-207}$ may bind 14-3-3ζ only weakly, it still effectively competes for the 14-3-3 binding groove with the N-terminal phosphopeptide of a second $dpAANAT_{1-207}$ molecule, perhaps by virtue of its proximity.

To determine if the postulated interaction between the C-terminal PKA site and 14-3-3ζ is structurally reasonable, we computationally extended the C terminus of $pAANAT_{1-201}$ to the end, and included pSer-205. The C terminus of $dpAANAT_{1-207}$ fits easily into the second 14-3-3 binding groove without the need to invoke any changes in the observed interactions between $pAANAT_{1-201}$ and the other 14-3-3 monomer.

Conclusions

The structure presented here allows us to describe in detail how serotonin N-acetyltransferase interacts with 14-3-3ζ. Our data suggest that AANAT may have evolved to recruit 14-3-3 to regulate its enzymatic activity in a phosphorylation-dependent manner, because the PKA/14-3-3 motif is absent in lower forms (Coon et al., 1995). This regulation is achieved by binding to 14-3-3, which structurally modulates the substrate binding sites, leading to measurable effects on the affinity of AANAT for its substrates with an accompanying increase in activity at low substrate concentrations.

The observed effect of 14-3-3 binding on the catalytic properties of AANAT is likely to be physiologically important. One possibility is that it improves the efficiency of AANAT by lowering its Km values. This would enable the enzyme to efficiently acetylate lower concentrations of serotonin, which is of special importance because the levels of serotonin in the pineal decrease 10-fold at night (Namboodiri et al., 1985). In sheep, serotonin concentrations vary from ~10 μM during the day to ~1 μM at night, values that are considerably lower than the Km value of 240 μM for the uncomplexed enzyme (De Angelis et al., 1998). Complex formation with 14-3-3 may also indicate a way for an enzyme to adapt to an environment in which its substrate concentrations oscillate over time. It is tempting to speculate that this approach might be preferable to adaptation through mutation, which would necessarily result in an enzyme that would work more efficiently at one substrate concentration versus the other, but without the flexibility to cycle between states. Another possibility is that complex formation could contribute to the dynamic changes in melatonin production by acting as a cAMP-regulated switch. It would be interesting to determine if the phosphorylation state of Thr-31 or Ser-205 varies as a function of the circadian cycle.

The structure presented here is consistent with the possibility that a third as-yet unidentified protein could occupy the second 14-3-3ζ binding site to further regulate AANAT activity in pineal cells. We observe two molecules of $pAANAT_{1-201}$ bound within the 14-3-3ζ dimer channel, providing structural insight into two models that have been proposed for 14-3-3 action. The first structures of dimeric 14-3-3 immediately suggested the possibility of simultaneously binding two different proteins (Liu et al., 1995; Xiao et al., 1995), an idea now supported by biochemical data (Braselmann and McCormick, 1995; Guthridge et al., 2000; MacNicol et al., 2000). The structure of the complex demonstrates one possible three-dimensional arrangement for two protein molecules bound to a 14-3-3 dimer in a phosphorylation-dependent and structurally defined manner. Another model of 14-3-3 action has been proposed for proteins possessing multiple 14-3-3 recognition sequences, for example Raf-1 (Muslin et al., 1996) and Cbl (Liu et al., 1997). Our model of the 14-3-3ζ:$dpAANAT_{1-207}$ complex demonstrates that the simultaneous binding of two sites within a single protein can be accommodated by the 14-3-3 inner channel.

Our structural results are likely to be broadly relevant in understanding the architecture of complexes formed by 14-3-3 with other binding partners. The extended

and rigid interface between 14-3-3ζ and $pAANAT_{1–201}$ demonstrates that 14-3-3 molecules can bind partners in a structurally reproducible manner, as opposed to merely tethering them at a single site (i.e., the phosphorylated residue) and allowing them to flop around in solution. This would appear to be the preferred means of binding a wide range of proteins whose subsequent function may require precise docking to other proteins. Finally, a large portion of the interactions holding AANAT within the central channel of the 14-3-3 dimer are remote from the phosphorylated residue. This may be a general feature of protein binding by 14-3-3, as it provides ample opportunity for conformational modulation.

Experimental Procedures

Expression, Purification, and Phosphorylation of AANAT

The expression construct for ovine $AANAT_{1–207}$ was prepared as described previously (Hickman et al., 1999a). Ovine $AANAT_{1–201}$ was a gift of A. B. Hickman. $AANAT_{1–201}$ and $AANAT_{1–207}$ were expressed as GST-fusion proteins and purified as described (Hickman et al., 1999a). The fusion proteins were cleaved by adding 5 U thrombin (Sigma) per mg protein, and the reactions monitored by SDS-PAGE. After removal of GST and thrombin, purified proteins were dialyzed overnight against buffer 1 (20 mM Tris [pH 7.5], 0.5 M NaCl, 1 mM EDTA, 5 mM DTT, and 10% [w/v] glycerol) prior to concentrating to ~2 mg/ml.

Purified AANAT (70 mg) in buffer 1 with 0.75 mM ATP and 15 mM $MgCl_2$ was phosphorylated by incubation with 5000 U of PKA (Promega) for 6 hr at 4°C. The reaction was stopped by the addition of EDTA (final concentration 15 mM). The completeness of the reaction was confirmed by IEF and electrospray mass spectrometry (ESI-MS) using a Quattro LC triple quadrupole electrospray mass spectrometer (Micromass, UK).

The final step, size-exclusion chromatography on TSK-Gel G3000SW, was performed in buffer 1. Purified proteins were characterized by SDS-PAGE, IEF, and mass spectrometry. We obtained a molecular mass of 22,298 Da (calc = 22,295 Da) for $pAANAT_{1–201}$, and 23,157 Da (calc = 23,159 Da) for $dpAANAT_{1–207}$.

Expression and Purification of 14-3-3ζ

DNA encoding human 14-3-3ζ (S. G. and D. C. K., unpublished data) was ligated into pET-15b (Novagen) using the NdeI and BamHI sites. The histidine-tagged protein was expressed by IPTG induction for 5 hr at 37°C and purified from *E. coli* BL21(DE3) using Chelating Sepharose according to the manufacturer's instructions (Amersham Pharmacia Biotech). The histidine tag was cleaved by incubation (6 hr at 15°C) with 10 U thrombin per mg protein. After cleavage, 14-3-3ζ was purified by anion-exchange chromatography on a HQ/M 4.6 × 100 column (PerSeptive Biosystems). The 14-3-3ζ was eluted using a 5–600 mM NaCl gradient in 50 mM Tris (pH 8.0), 1 mM DTT. Fractions containing 14-3-3ζ were dialyzed overnight against buffer 2 (20 mM Tris [pH 7.5], 1 mM EDTA, 5 mM DTT, and 10% [w/v] glycerol) prior to concentrating to ~4 mg/ml. Purified 14-3-3ζ was characterized by SDS-PAGE, IEF, and MALDI-TOF mass spectrometry using a PerSeptive Biosystems Voyager-DE instrument.

Analytical gel filtration experiments to monitor complex formation were performed on a Pharmacia SmartSystem Superdex 75 column equilibrated at 4°C.

Gel Filtration of 14-3-3ζ:pAANAT-Derived Phosphopeptide Complexes

The association of AANAT-derived phosphopeptides with 14-3-3ζ was assessed by gel filtration in buffer 2. Phosphorylated peptides were obtained from PeptidoGenic Research (Livermore, CA), and were HPLC-purified and characterized by MS. The phosphopeptide corresponding to the N-terminal region of pAANAT (residues 19–38, GIPGSPGRQRRHpTLPANEWR, where Phe-37 was replaced by Trp to increase the absorption at 280 nm) comigrated with 14-3-3ζ, while the C-terminal phosphopeptide (residues 188–207, WTEMHC SLRGHAALRRNpSDR, where Phe-188 was replaced by Trp) did not. Fractions were analyzed using SDS-PAGE.

Crystallization, Data Collection, and Structure Determination

$pAANAT_{1–201}$ (23 μM), 14-3-3ζ (46 μM), and the bisubstrate analog (70 μM), a gift of the NIMH Chemical Synthesis Program (RBI, Natick, MA), were combined and dialyzed overnight against 20 mM Tris (pH 7.5), 20 mM Li_2SO_4, 5 mM DTT, 1 mM EDTA, and 10% (w/v) glycerol prior to concentrating to ~5 mg/ml. Clusters of very thin plates grew in 4–6 weeks at 4°C in hanging drops consisting of a 1:1 mixture of the complex and a well solution consisting of 20 mM Tris (pH 7.5), 30% (w/v) PEG 4000, and 20 mM $MgCl_2$. After disruption of the clusters, single crystals were transferred into a stabilization solution consisting of 20 mM Tris (pH 7.5), 10 mM Li_2SO_4, 2.5 mM DTT, 0.5 mM EDTA, 5% (w/v) glycerol, 15% (w/v) PEG 4000, and 10 mM $MgCl_2$. The glycerol concentration was slowly increased to 20%, and crystals were frozen by rapid immersion in liquid propane.

Data were collected at 95 K on a Raxis II image plate detector mounted on a Rigaku RU-200 rotating anode source operated at 50 kV/100 mA with double mirror-focused Cu Kα radiation. The crystals belong to the space group P1 with cell dimensions a = 74.72 Å, b = 75.08 Å, c = 101.78 Å, α = 90.14°, β = 90.06°, and γ = 63.04°, and have a solvent content of 53.5%. There are two complexes with 2:2 stoichiometry in the asymmetric unit. Data were integrated and scaled internally using the HKL suite (Otwinowski and Minor, 1997).

The crystal structure was solved by molecular replacement using AMoRe (Navaza and Saludjian, 1997). Two search models were used, 14-3-3ζ (Liu et al., 1995; PDB code 1a4o) and $AANAT_{28–201}$ complexed with the bisubstrate analog (Hickman et al., 1999b; PDB code 1cjw). The cross-rotation solutions for the two 14-3-3ζ dimers had linear correlation coefficients of 13.4% and 13.0%, and for the four $AANAT_{28–201}$ molecules, 17.7%, 17.0%, 15.0%, and 14.6%, respectively. The translation solution with all eight molecules placed had a crystallographic R factor of 46.3%. Further rigid body, molecular dynamics, energy minimization, and B factor refinement were carried out with XPLOR 3.1 (Brünger, 1992a) and CNS (Brünger et al., 1998). Noncrystallographic symmetry (NCS) restraints were imposed between all four molecules of pAANAT, 14-3-3ζ and the bisubstrate analog. R_{free} was used to determine the best weight for NCS; 150 kcal/mol was used throughout. Five percent of the data, randomly selected, was used exclusively to monitor the free R factor (Brünger, 1992b). Bulk solvent correction was used as well as the TNT B factor restraint library (Tronrud, 1996). Difference electron density for the N terminus (from Ser-18) of pAANAT with phosphothreonine was clearly visible even at the early stages. In the current model, 91.0% of all residues are in the most favored region of the Ramachandran plot and none in the disallowed region; in the final stages of the refinement, 239 solvent molecules were included. Figures 1 and 3 were generated using RIBBONS (Carson, 1991). The surfaces in Figure 2 were computed with MS (Connolly, 1983) and SPOCK (Christopher, 1998); the molecules were drawn with Molscript (Kraulis, 1991) and rendered with Povray (www.povray.org) run on a Beowulf cluster (biowulf.nih.gov).

Analytical Ultracentrifugation

Analytical ultracentrifugation experiments were performed using a Beckman XL-A analytical ultracentrifuge as previously described (Ghirlando et al., 1995). Sedimentation equilibrium experiments at loading concentrations of 14 to 30 μM, were conducted at 4.0°C and rotor speeds of 8,000, 10,000, and 12,000 rpm. Proteins were dialyzed against buffer 3 (50 mM sodium citrate [pH 6.5] and 5 mM 2-mercaptoethanol) or buffer 4 (20 mM Tris [pH 7.5], 1 mM EDTA, 5 mM 2-mercaptoethanol, and 10% (w/v) glycerol). $pAANAT_{1–201}$ and 14-3-3ζ were monodisperse in both buffers and data analysis in terms of a single ideal solute (Ghirlando et al., 1995) led to the buoyant molecular mass, $M(1-\nu\rho)$. $pAANAT_{1–201}$ was monomeric and 14-3-3ζ was dimeric. 2:1 and 2:2 mixtures of 14-3-3ζ and $pAANAT_{1–201}$ in buffer 4 yielded monodisperse species corresponding to complete 2:1 and 2:2 complex formation, respectively. Data for the 2:1 mixture were not compatible with an equimolar mix of 2:2 complexes and free 14-3-3ζ dimers. Using a 4:3 loading mixture of 14-3-3ζ: $pAANAT_{1–201}$, data were best modeled in terms of an equimolar mix

of 2:2 and 2:1 complexes. Whereas a 2:1 mixture of 14-3-3ζ and dpAANAT$_{1–207}$ was best modeled in terms of a 2:1 complex, no evidence for 2:2 complexes was noted at a 2:2 loading mixture.

2:1 and 2:2 mixtures of 14-3-3ζ:pAANAT$_{1–201}$ in buffer 3 yielded data that were the best modeled in terms of reversible 2:1 and 2:2 complex formation. Simultaneous weighted nonlinear least squares fitting (Shi et al., 1997) led to values for $K_1 = K_2$ and $K_1(2) = K_2(1)$. K_1 values (K_{D1} = 20 nM) were such that 2:1 complex formation is essentially complete. The $K_{D2}(1)$ value was 70 μM. In all cases, a random distribution of the residuals from zero was noted as a function of the radius.

Isothermal Titration Calorimetry

Binding of substrates to pAANAT alone and in complex with 14-3-3ζ was measured by isothermal titration calorimetry (Wiseman et al., 1989) using an MCS titration calorimeter (MicroCal Inc., Northampton, MA). Aliquots of 5 μl 20 mM AcCoA or serotonin were titrated at 22°C by injection into protein (12–15 μM in 1.347 ml) in 20 mM Na-citrate (pH 7.0), 5 mM DTT, and 1 mM EDTA. The titration with 20 mM serotonin was performed in the presence of 5 mM CoA to avoid enzyme turnover. After subtraction of dilution heats, calorimetric data were analyzed using the Origin package, version 2.9. Dissociation constants ($K_D = 1/K_a$), Gibbs free energy changes ($\Delta G = -RT \ln K_a$), and entropy changes ($\Delta S = \Delta H/T - \Delta G/T$) at 295 K were calculated from ΔH and K_a values.

The binding isotherms for AcCoA titrations could not be fit using a single binding site model. The best fit was obtained using a two independent site model where the second binding constant was in the range 2–5 mM, and likely reflects an artifact due to AcCoA oligomerization prior to injection (Bijma et al., 1994).

Enzyme Activity Measurements

The activities of pAANAT$_{1–201}$ and dpAANAT$_{1–207}$ were measured using the colorimetric assay essentially as described by De Angelis et al. (1998). The assay was performed at 22°C in buffer containing 20 mM sodium citrate (pH 7.0), 300 mM NaCl, 1 mM EDTA, 0.05 mg/ml BSA, 50 μM AcCoA, and 20 μM serotonin. The reaction was started by the addition of enzyme (23 nM) and variable amounts of 14-3-3ζ. When pAANAT$_{1–201}$ was assayed alone under conditions similar to those of De Angelis et al., 1998 (20 mM sodium citrate [pH 7.0] and 500 mM NaCl at 30°C) using serotonin as a substrate, Km(app) = 183 μM and K_{cat}(app) = 33.3 s^{-1}, in good agreement with published data.

Acknowledgments

We thank Alison Burgess Hickman for her help at all stages of this project, and acknowledge helpful discussions with members of the Klein lab. We also thank Eric Anderson for ESI-MS measurements, Susan Chacko for assistance with graphics, and Alison Burgess Hickman and David R. Davies for critical reading of the manuscript.

Received December 20, 2000; revised February 27, 2001.

References

Aitken, A. (1996). 14-3-3 and its possible role in co-ordinating multiple signalling pathways. Trends Cell Biol. *6*, 341–347.

Arendt, J. (1995). Melatonin and the Mammalian Pineal Gland. (London: Chapman and Hall).

Banik, U., Wang, G.-A., Wagner, P.D., and Kaufman, S. (1997). Interaction of phosphorylated tryptophan hydroxylase with 14-3-3 proteins. J. Biol. Chem. *272*, 26219–26225.

Bijma, K., Engberts, J.B.F.N., Haandrikman, G., van Os, N.M., Blandamer, M.J., Butt, M.D., and Cullis, P.M. (1994). Thermodynamics of micelle formation by 1-methyl-4-alkylpyridinium halides. Langmuir *10*, 2578–2582.

Boston, P.F., Jackson, P., Kynoch, P.A.M., and Thompson, R.J. (1982). Purification, properties, and immunohistochemical localization of human brain 14-3-3 protein. J. Neurochem. *38*, 1466–1474.

Braselmann, S., and McCormick, F. (1995). Bcr and Raf form a complex in vivo via 14-3-3 proteins. EMBO J. *14*, 4839–4848.

Brunet, A., Bonni, A., Zigmond, M.J., Lin, M.Z., Juo, P., Hu, L.S., Anderson, M.J., Arden, K.C., Blenis, J., and Greenberg, M.E. (1999). Akt promotes cell survival by phosphorylating and inhibiting a Forkhead transcription factor. Cell *96*, 857–868.

Brünger, A.T. (1992a). X-PLOR Version 3.1. A system for X-ray crystallography and NMR. (New Haven, CT: Yale University Press).

Brünger, A.T. (1992b). Free R value: a novel statistical quantity for assessing the accuracy of crystal structures. Nature *355*, 472–475.

Brünger, A.T., Adams, P.D., Clore, G.M., Delano, W.L., Gros, P., Grosse-Kunstleve, R.W., Jiang, J.-S., Kuszewski, J., Nilges, N., Pannu, N.S., et al. (1998). Crystallography and NMR System (CNS): a new software system for macromolecular structure determination. Acta Crystalogr. *D54*, 905–921.

Carson, M. (1991). RIBBONS 2.0. J. Appl. Crystallogr. *24*, 958–961.

Christopher, J.A. (1998). SPOCK: the structural properties observation and calculation kit (program manual), The Center for Macromolecular Design, Texas A&M University, College Station, TX.

Connolly, M.L. (1983). Solvent-accessible surfaces of proteins and nucleic acids. Science *221*, 709–713.

Coon, S.L., Roseboom, P.H., Baler, R., Weller, J.L., Namboodiri, M.A.A., Koonin, E.V., and Klein, D.C. (1995). Pineal serotonin N-acetyltransferase: Expression cloning and molecular analysis. Science *270*, 1681–1683.

De Angelis, J., Gastel, J., Klein, D.C., and Cole, P.A. (1998). Kinetic analysis of the catalytic mechanism of serotonin N-acetyltransferase (EC 2.3.1.87). J. Biol. Chem. *273*, 3045–3050.

Dunlap, J.C. (1999). Molecular bases for circadian clocks. Cell *96*, 271–290.

Dyda, F., Klein, D.C., and Hickman, A.B. (2000). GCN5-related N-acetyltransferases: A structural overview. Annu. Rev. Biophys. Biomol. Struct. *29*, 81–103.

Finnie, C., Borch, J., and Collinge, D.B. (1999). 14-3-3 proteins: eukaryotic regulatory proteins with many functions. Plant Mol. Biol. *40*, 545–554.

Fu, H., Subramanian, R.R., and Masters, S.C. (2000). 14-3-3 proteins: Structure, function, and regulation. Annu. Rev. Pharmacol. Toxicol. *40*, 617–647.

Gastel, J.A., Roseboom, P.H., Rinaldi, P.A., Weller, J.L., and Klein, D.C. (1998). Melatonin production: proteasomal proteolysis in serotonin N-acetyltransferase regulation. Science *279*, 1358–1360.

Ghirlando, R., Keown, M.B., Mackay, G.A., Lewis, M.S., Unkeless, J.C., and Gould, H.J. (1995). Stoichiometry and thermodynamics of the interaction between the Fc fragment of human IgG_1 and its low-affinity receptor FcγRIII. Biochem. *34*, 13320–13327.

Guthridge, M.A., Stomski, F.C., Barry, E.F., Winnall, W., Woodcock, J.M., McClure, B.J., Dottore, M., Berndt, M.C., and Lopez, A.F. (2000). Site-specific serine phosphorylation of the IL-3 receptor is required for hemopoietic cell survival. Mol. Cell *6*, 99–108.

Hickman, A.B., Klein, D.C., and Dyda, F. (1999a). Melatonin biosynthesis: The structure of serotonin N-acetyltransferase at 2.5 Å resolution suggests a catalytic mechanism. Mol. Cell *3*, 23–32.

Hickman, A.B., Namboodiri, M.A.A., Klein, D.C., and Dyda, F. (1999b). The structural basis of ordered substrate binding by serotonin N-acetyltransferase: Enzyme complex at 1.8 Å resolution with a bisubstrate analog. Cell *97*, 361–369.

Hinz, H.-J. (1983). Thermodynamics of protein-ligand interactions: Calorimetric approaches. Annu. Rev. Biophys. Bioeng. *12*, 285–317.

Khalil, E.M., and Cole, P.A. (1998). A potent inhibitor of the melatonin rhythm enzyme. J. Am. Chem. Soc. *120*, 6195–6196.

Klein, D.C., Moore, R.Y., and Reppert, S.M., eds. (1991). Suprachiasmatic Nucleus: The Mind's Clock. (New York: Oxford University Press).

Klein, D.C., Coon, S.L., Roseboom, P.H., Weller, J.L., Bernard, M., Gastel, J.A., Zatz, M., Iuvone, P.M., Rodriguez, I.R., Begay, V., et al. (1997). The melatonin rhythm-generating enzyme: molecular regulation of serotonin N-acetyltransferase in the pineal gland. Recent Prog. Horm. Res. *52*, 307–358.

Klein, D.C., Baler, R., Rosenboom, P.H., Weller, J.L., Bernard, M.,

Gastel, J.A., Zatz, M., Iuvone, P.M., Begay, V., Falcon, J., et al. (1998). The molecular basis of the pineal melatonin rhythm: Regulation of serotonin N-acetylation. In Handbook of Behavioral State Control, R. Lydic and H. Baghdoyan, eds. (Boca Raton, FL: CRC Press), pp. 45–59.

Kraulis, P.J. (1991). MOLSCRIPT: a program to produce both detailed and schematic plots of protein structures. J. Appl. Crystallogr. *24*, 946–950.

Liu, D., Bienkowska, J., Petosa, C., Collier, R.J., Fu, H., and Liddington, R. (1995). Crystal structure of the zeta isoform of the 14-3-3 protein. Nature *376*, 191–194.

Liu, Y.-C., Liu, Y., Elly, C., Yoshida, H., Lipkowitz, S., and Altman, A. (1997). Serine phosphorylation of Cbl induced by phorbol ester enhances its association with 14-3-3 proteins in T cells via a novel serine-rich 14-3-3-binding motif. J. Biol. Chem. *272*, 9979–9985.

MacNicol, M.C., Muslin, A.J., and MacNicol, A.M. (2000). Disruption of the 14-3-3 binding site within the B-Raf kinase domain uncouples catalytic activity from PC12 cell differentiation. J. Biol. Chem. *275*, 3803–3809.

Muslin, A.J., Tanner, J.W., Allen, P.M., and Shaw, A.S. (1996). Interaction of 14-3-3 with signaling proteins is mediated by the recognition of phosphoserine. Cell *84*, 889–897.

Namboodiri, M.A.A., Sugden, D., Klein, D.C., Tamarkin, L., and Mefford, I.N. (1985). Serum melatonin and pineal indoleamine metabolism in a species with a small day/night N-acetyltransferase rhythm. Comp. Biochem. Physiol. *80B*, 731–736.

Navaza, J., and Saludjian, P. (1997). AMoRe: An automated molecular replacement program package. Methods Enzymol. *276*, 581–594.

Neuwald, A.F., and Landsman, D. (1997). GCN5-related histone N-acetyltransferases belong to a diverse superfamily that includes the yeast SPT10 protein. Trends Biochem. Sci. *22*, 154–155.

Otwinowski, Z., and Minor, W. (1997). Processing of X-ray diffraction data collected in oscillation mode. Methods Enzymol. *276*, 307–326.

Petosa, C., Masters, S.C., Bankston, L.A., Pohl, J., Wang, B., Fu, H., and Liddington, R.C. (1998). 14-3-3ζ binds a phosphorylated Raf peptide and an unphosphorylated peptide via its conserved amphipathic groove. J. Biol. Chem. *273*, 16305–16310.

Reppert, S.M. (1998). A clockwork explosion! Neuron *21*, 1–4.

Rittinger, K., Budman, J., Xu, J., Volinia, S., Cantley, L.C., Smerdon, S.J., Gamblin, S.J., and Yaffe, M.B. (1999). Structural analysis of 14-3-3 phosphopeptide complexes identifies a dual role for the nuclear export signal of 14-3-3 in ligand binding. Mol. Cell *4*, 153–166.

Roseboom, P.H., Weller, J.L., Babila, T., Aitken, A., Sellers, L.A., Moffett, J.R., Namboodiri, M.A.A., and Klein, D.C. (1994). Cloning and characterization of the ϵ and ζ isoforms of the 14-3-3 proteins. DNA Cell Biol. *13*, 629–640.

Roseboom, P.H., Coon, S.L., Baler, R., McCune, S.K., Weller, J.L., and Klein, D.C. (1996). Melatonin synthesis: analysis of the more than 150-fold nocturnal increase in serotonin N-acetyltransferase messenger ribonucleic acid in the rat pineal gland. Endocrinol. *137*, 3033–3045.

Shi, J., Ghirlando, R., Beavil, R.L., Beavil, A.J., Keown, M.B., Young, R.J., Owens, R.J., Sutton, B.J., and Gould, H.J. (1997). Interaction of the low-affinity receptor CD23/FcϵRII lectin domain with the Fcϵ3–4 fragment of human immunoglobulin E. Biochem. *36*, 2112–2122.

Sutherland, G.R.J., and Aust, S.D. (1997). Thermodynamics of binding of the distal calcium to manganese peroxidase. Biochem. *36*, 8567–8573.

Tanji, M., Horwitz, R., Rosenfeld, G., and Waymire, J.C. (1994). Activation of protein kinase C by purified bovine brain 14-3-3: comparisom with tyrosine hydroxylase activation. J. Neurochem. *63*, 1908–1916.

Thibault, C., Falcon, J., Greenhouse, S.E., Lowery, C.A., Gern, W.A., and Collin, J.P. (1993). Regulation of melatonin production by pineal photoreceptor cells—role of cyclic-nucleotides in the trout. J. Neurochem. *61*, 332–339.

Thorson, J.A., Yu, L.W.K., Hsu, A.L., Shih, N.Y., Graves, P.R., Tanner, J.W., Allen, P.M., Piwnica-Worms, H., and Shaw, A.S. (1998). 14-3-3 proteins are required for maintenance of Raf-1 phosphorylation and kinase activity. Mol. Cell. Biol. *18*, 5229–5238.

Tronrud, D.E. (1996). Knowledge-based B-factor restraints for the refinement of proteins. J. Appl. Crystallogr. *29*, 100–104.

Vincenz, C., and Dixit, V.M. (1996). 14-3-3 proteins associate with A20 in an isoform-specific manner and function both as chaperone and adapter molecules. J. Biol. Chem. *271*, 20029–20034.

Wiseman, T., Williston, S., Brandts, J.F., and Lin, L.N. (1989). Rapid measurement of binding constants and heats of binding using a new titration calorimeter. Anal. Biochem. *179*, 131–137.

Xiao, B., Smerdon, S.J., Jones, D.H., Dodson, G.G., Soneji, Y., Aitken, A., and Gamblin, S.J. (1995). Structure of a 14-3-3 protein and implications for coordination of multiple signalling pathways. Nature *376*, 188–191.

Yaffe, M.B., Rittinger, K., Volinia, S., Caron, P.R., Aitken, A., Leffers, H., Gamblin, S.J., Smerdon, S.J., and Cantley, L.C. (1997). The structural basis for 14-3-3:phosphopeptide binding specificity. Cell *91*, 961–971.

Protein Data Bank Accession Number

The coordinates have been deposited with the Protein Data Bank (accession number 1IB1).